Journal of Plant Growth Regulation (2026) 45:3052–3062
https://doi.org/10.1007/s00344-026-12054-w

Redox Dynamics Modulate Vascular Tissue Reconnection and Early Growth after Grafting in *Pyrus* and*Cydonia*

Evaldo Tadeu de Melo[1] · Rafael Pio[2] · Daniela da Hora Farias[3] · Alexandre Dias da Silva[1] · Evaristo Mauro de Castro[2] · Carlos Henrique Milagres Ribeiro[2]

Received: 29 October 2025 / Accepted: 8 January 2026 / Published online: 9 March 2026
© The Author(s) 2026

Abstract

Graft success depends on coordinated vascular tissue regeneration to restore scion growth. Reactive oxygen species (ROS), particularly hydrogen peroxide (H_2O_2), are involved in wound signalling, yet their role in controlling intergeneric graft compatibility remains unclear. This study evaluated early growth, redox metabolism and vascular reconnection in intergeneric grafts between quince (*Cydonia oblonga*) and pear (*Pyrus* spp.). A completely randomised 2 × 8 factorial scheme was adopted, comprising two rootstocks (*Pyrus calleryana* and *Chaenomeles sinensis*) and eight scion genotypes. Sprouting percentage, shoot length and diameter, hydrogen peroxide (H_2O_2) concentration, malondialdehyde (MDA) content and anatomical reconnection were assessed up to 120 days after grafting. Compatible combination exhibited markedly higher sprouting and shoot growth; for instance, 'Triunfo' reached 100% sprouting on *P. calleryana*, whereas *P. calleryana* on *C. sinensis* failed completely (0%), and *C. sinensis* on *P. calleryana* showed only about 10% sprouting. Callus formation was detected as early as 5 days after grafting (DAG), and continuous vascular connections were established by 25 DAG in compatible grafts, while incompatible combinations developed necrotic barriers at the graft interface. H_2O_2 concentration in the graft region ranged from approximately 261 to 579 nmol g^{-1} FW and was generally higher in scion tissues, whereas MDA accumulation was greater in rootstocks, reaching up to around 560 µmol MDA g^{-1} FW. Although single point oxidative markers did not strictly discriminate compatible from incompatible combinations, tissue-specific redox patterns and their timing were consistently associated with the speed of vascular reconnection and early scion growth. These findings demonstrate that ROS function not only as stress markers but also as developmental signals during graft healing, and suggest early vascular reconnection together with scion H_2O_2 and rootstock MDA as promising indicators of graft performance in woody species.

Keywords Oxidative metabolism · Vascular differentiation · Wound signaling · Graft healing · Pyrus · Cydonia

Introduction

In European regions, pear (*Pyrus* spp.) propagation is predominantly performed through grafting onto quince (*Cydonia* spp.) rootstocks (Öztürk 2021). However, *Cydonia* rootstocks often exhibit poor adaptation to tropical and subtropical environments due to their sensitivity to high soil temperatures and limited tolerance to acidic soils (Darshan and Solanki 2022).

The use of *Pyrus* rootstocks for commercial pear cultivars provides advantages such as better adaptation to warm climates and resistance to fire blight (*Erwinia amylovora*) (Kurt et al. 2023). Meanwhile, *Chaenomeles sinensis* a quince species closely related to *Cydonia* has shown potential as a rootstock for both quince and pear, potentially

Communicated by Dongdong Li.

✉ Carlos Henrique Milagres Ribeiro
chm.ribeiro8@gmail.com

[1] Federal Institute of Southern Minas Gerais – Inconfidentes Campus, Tiradentes Square, Code, Inconfidentes 37576-000, MG, Brazil

[2] Agricultural Research of Minas Gerais – EPAMIG Leopoldina Campus, Airport Road, via rural área, Code, Leopoldina 36700-000, MG, Brazil

[3] Federal University of Lavras (UFLA), Aguenta Sol, Code, Lavras 37200-900, MG, Brazil

overcoming some limitations associated with traditional rootstocks (Milagres et al. 2023). This approach could enable the establishment of higher-density and more resilient orchards (Ozturk and Faizi 2023). Nevertheless, the compatibility of *Pyrus* and *Chaenomeles* graft combinations remains poorly understood.

The degree of graft compatibility is closely linked to the genetic proximity between scion and rootstock (Ashraf et al. 2025). While autografts are fully compatible, intergeneric combinations often show incomplete or delayed vascular reconnection (Habibi et al. 2022; Loupit et al. 2023). Recent research has highlighted that graft compatibility involves not only anatomical alignment but also complex physiological and signaling processes that regulate tissue adhesion and vascular differentiation (Wang et al. 2024). Among these, the redox signaling network plays a central role during the healing of graft wounds and the establishment of functional connections between partners (Nie and Wen 2023).

Reactive oxygen species (ROS) such as hydrogen peroxide (H_2O_2) are key components of this network. At moderate levels, ROS act as secondary messengers that trigger defense responses and promote tissue regeneration, whereas excessive accumulation leads to oxidative stress and programmed cell death (Anjum et al. 2022). Thus, the balance between ROS generation and scavenging determines whether oxidative metabolism contributes to successful signaling and vascular reconnection or to tissue damage and incompatibility (Tan et al. 2023). Hydrogen peroxide, due to its relatively long half-life and high membrane permeability, is considered a primary mediator of redox-dependent signaling in plants (Hong et al. 2024). Conversely, excessive peroxidation of membrane lipids results in the accumulation of malondialdehyde (MDA), which reflects oxidative injury and cell death (Yuan et al. 2024).

Despite growing recognition of ROS as signaling molecules in graft healing, few studies have explicitly linked redox signaling to the anatomical reconnection of vascular tissues in intergeneric combinations of fruit trees. Understanding this relationship is crucial for elucidating the biochemical and signaling mechanisms underlying graft compatibility. In this context, the present study aimed to correlate antioxidant metabolism and vascular tissue reconnection in intergeneric combinations of quince and pear, with an emphasis on the role of redox signaling in modulating graft compatibility.

Here, we hypothesize that temporally regulated redox signalling at the graft interface not only mediates wound healing but actively modulates the developmental programs that govern vascular differentiation and subsequent scion growth. Demonstrating this link will inform broader models of growth regulation in woody plants.

Materials and Methods

Experimental Site and Plant Material

The experiment was carried out at the Fruit Growing Sector of the Department of Agriculture of the Federal University of Lavras (UFLA), located in Lavras, Minas Gerais, Brazil (21°14′S, 45°00′W, 918 m altitude). The region has a Cwa climate (humid subtropical with dry winters), according to the Köppen classification.

Seeds of the rootstocks *Pyrus calleryana* and *Chaenomeles sinensis* were extracted from mature fruits collected at the São Bento do Sapucaí Seedling Production Center, managed by the Technical and Integral Assistance Coordination (CATI) of São Paulo State. The seeds were manually cleaned, dried, and subjected to stratification in moist sand at 4 °C for 60 days to overcome dormancy. After stratification, the seeds were sown in 72-cell polypropylene trays (120 cm^3 per cell) filled with medium-grade expanded vermiculite, following the recommendations of Seifert et al. (2009).

Seedling Growth and Grafting Procedure

After 60 days of emergence, uniform seedlings were transplanted into 1.5 dm^3 polyethylene bags containing a substrate composed of subsoil, sand, and organic compost in a 2:1:1 (v/v/v) ratio, enriched with 5 $g \cdot dm^{-3}$ of a simple NPK fertilizer (4–14-8). The seedlings were grown under a 50% shade structure and trained to maintain a single stem.

Cleft grafting was performed when seedlings reached approximately 7 mm stem diameter and 15 cm height. Scion cuttings were collected from quince (*Cydonia oblonga*) and pear (*Pyrus spp.*) collections at UFLA, standardized to 10 cm in length and 7 mm in diameter.

The rootstocks (*P. calleryana* and *C. sinensis*) were grafted with eight scion types: pear cultivars ‘Packham’s Triumph’, ‘William’s’, ‘Triunfo’, ‘Primorosa’, and ‘Shenseri’; the quince cultivar ‘Mendoza Inta 37’; and the species *P. calleryana* and *C. sinensis*.

The experimental design was completely randomized in a 2 × 8 factorial scheme (two rootstocks × eight scions), with three replications and 15 grafts per plot.

After grafting, the unions were wrapped with transparent polyethylene tape and covered with polyethylene bags (15 × 20 cm) to maintain high humidity and prevent desiccation. After 30 days, the bags were removed, and 60 days after grafting, the tapes were carefully detached to avoid mechanical damage.

Growth Evaluation

Seedlings were maintained under 50% shade and irrigated daily to keep the substrate moist. Rootstock suckers and unwanted shoots were periodically removed to ensure uniform growth.

At 120 days after grafting (DAG), the following parameters were evaluated:

- Sprouting percentage (%): grafts were considered sprouted when buds exhibited developed leaves;
- Shoot length (cm): measured from the base of the scion to the apex;
- Shoot diameter (mm): measured 1 cm above the graft union using a digital caliper.

Biochemical Analyses and Redox Signaling

To assess the oxidative balance and redox signaling during graft union formation, biochemical analyses were conducted at the Laboratory of Biochemistry and Molecular Physiology, Department of Biology, UFLA.

Samples were collected from the graft interface (1 cm above and 1 cm below the union) at 5, 15, 25, 35, and 45 days after grafting, using three seedlings per treatment per time point. Each sample was immediately frozen in liquid nitrogen and stored at −80 °C until analysis.

For each collection, samples were separated into scion and rootstock tissues. Considering two rootstocks, eight scions, five sampling times, three replications, and two tissue portions per seedling, a total of 480 samples were analyzed in duplicate.

Approximately 200 mg of tissue were ground in liquid nitrogen with polyvinylpolypyrrolidone (PVPP) and homogenized in 1.5 mL of 0.1% (w/v) trichloroacetic acid (TCA). The homogenate was centrifuged at 12,000 g for 15 min at 4 °C, and the supernatant was used for the following analyses:

- Hydrogen peroxide (H_2O_2): quantified at 390 nm in a medium containing 10 mM potassium phosphate buffer (pH 7.0) and 1 M potassium iodide, according to Velikova et al. (2000). Quantification was performed using a standard curve of known H_2O_2 concentrations.
- Lipid peroxidation (malondialdehyde – MDA): determined via thiobarbituric acid-reactive substances (TBARS), following Buege and Aust (1978). A 125 µL aliquot of supernatant was mixed with a reaction solution containing 0.5% (w/v) thiobarbituric acid (TBA) and 10% (w/v) TCA. The mixture was heated at 95 °C for 30 min, cooled on ice, and absorbance was read at 535 and 600 nm. MDA concentration was calculated using the equation:

$$[MDA] = \frac{A_{535} - A_{600}}{\epsilon \times b}$$

where $\varepsilon = 1.56 \times 10^5$ $cm^{-1} \cdot M^{-1}$ (extinction coefficient) and $b = 1$ cm (path length).

Anatomical Characterization and Vascular Reconnection

Anatomical analyses were performed at the Wood Anatomy Laboratory, Department of Forest Sciences, UFLA. Samples were collected from the graft region (1 cm above and below the union) at 5, 15, 25, 35, and 45 days after grafting, using one seedling per treatment and time point, totaling 80 samples.

Samples were fixed in FAA 70% (formalin, glacial acetic acid, and 70% ethanol, 0.5:0.5:9, v/v/v) for 48 h and stored in 70% ethanol (Kraus and Arduin 1997). They were then dehydrated in an ethanol series (70%, 80%, 90%, and 100%), infiltrated in a 1:1 ethanol: resin mixture for 24 h, and embedded in Leica Historesin (hydroxyethyl methacrylate, Heidelberg, Germany).

Transverse Sect. (12 µm thick) were obtained using a Leica Jung SM 2000 rotary microtome, cleared in sodium hypochlorite (NaOCl) for 2 h, rinsed three times with distilled water, stained with 1% toluidine blue, and mounted in Verniz Vitral®.

Images were captured using a Zeiss optical microscope equipped with a digital camera. Rootstock thickness and callus mass area at the graft union were measured at four points per section using ImageJ software. These measurements were used to assess the extent of vascular reconnection and callus proliferation at different healing stages.

Statistical Analysis

Data were subjected to analysis of variance (ANOVA), and means were compared using the Scott-Knott test at a 5% probability level, employing the SISVAR software (Ferreira 2019).

Results

A significant interaction between rootstocks and cultivars was observed for sprouting percentage, shoot length, and shoot diameter (Table 1). In *Pyrus calleryana*, only *C. sinensis* exhibited a low sprouting rate (10%), while the cultivars ‘Triunfo’ and ‘Primorosa’ reached 100%. In *C.*

Table 1 Sprouting average, length and diameter of the cultivars of pear, Triunfo, Primorosa, packham's Triumph, william's and Shenseri cultivars, of the quince cultivar Mendoza Inta 37 and of the rootstocks themselves, at 120 days after grafting (DPE)

Cultivars	Sprout (%)*		Length (cm)	
	P. calleryana	C. sinensis	*P.* calleryana	C. sinensis
Triunfo	100.0 aA	90.0 aA	37.3 bA	3.0 cB
Primorosa	100.0 aA	33.3 cB	21.8 cA	6.0 cB
Packham's Triumph	89.0 aA	63.3 bB	20.3 cA	6.3 cB
William's	90.0 aA	69.0 bA	10.6 dA	3.6 cB
Shenseri	50.0 cA	53.3 bA	26.8 cA	3.1 cB
Mendoza Inta 37	90.0 aA	100.0 aA	47.4 aA	53.6 bA
C. sinensis	10.0 dB	90.0 aA	10.3 dB	73.1 aA
P. calleryana	66.6 bA	00 dB	34.1 bA	0.0 cB
CV (%)	16.74		29.23	

Cultivars	Diameter (mm)	
	P. calleryana	*C. sinensis*
Triunfo	4.4 bA	2.6 bB
Primorosa	4.1 bA	3.2 bA
Packham's Triumph	4.4 bA	3.3 bA
William's	3.8 bA	3.6 bA
Shenseri	5.7 aA	2.9 bB
Mendoza Inta 37	4.1 bA	4.9 aA
C. sinensis	1.3 cB	5.0 aA
P. calleryana	4.1 bA	0.0 bB
CV (%)	20.36	

* The averages followed by the same lowercase letter in the column and uppercase in the row within each variable belong to the same group by the Scott-Knott test at the 5% probability level

sinensis, the highest means were recorded for 'Mendoza Inta 37', 'Triunfo', and the self-graft combination. No sprouting occurred when *C. sinensis* was grafted onto *P. calleryana*, indicating total graft incompatibility. Comparing rootstocks, 'Triunfo' and 'Primorosa' showed superior performance on *P. calleryana*, whereas 'Mendoza Inta 37' performed best on *C. sinensis*.

A similar interaction pattern was found for shoot length. 'Mendoza Inta 37' exhibited the greatest shoot elongation across both rootstocks, followed by 'Triunfo' on *P. calleryana* and the self-graft on *C. sinensis* (Table 1). Only 'Mendoza Inta 37' maintained consistent growth performance on both rootstocks. No sprouting or growth was observed for *C. sinensis* grafted onto *P. calleryana*.

For shoot diameter, 'Shenseri' presented the highest values on *P. calleryana*, while the self-graft and 'Mendoza Inta 37' showed greater diameters on *C. sinensis* (Table 1). When comparing rootstocks, *C. sinensis* produced thicker shoots among self-grafts, while 'Triunfo' and 'Shenseri' developed larger diameters on *P. calleryana*.

Table 2 Means of hydrogen peroxide concentration and lipid peroxidation content of the five harvesting times, in the rootstock and the graft in the grafting region, of the *P. calleryana* and *C.sinensis* rootstocks grafted with the differents Pear cultivars

Cultivars	Hydrogen Peroxide rootstock (nM/g MF)*		Hydrogen Peroxide graft (nM/g MF)	
	P. calleryana	C. sinensis	*P.* calleryana	C. sinensis
Triunfo	98.47 aA	132.40 bA	460.66 aA	441.51 bA
Primorosa	86.53 aB	160.53 aA	509.49 aA	470.78 bA
Packham's Triumph	110.24 aA	119.67 bA	340.98 bA	285.92 cA
William's	67.24 aA	84.78 cA	301.95 bA	316.19 cA
Shenseri	111.04 aA	128.29 bA	567.34 aA	579.79 aA
Mendoza Inta 37	122.27 aA	156.19 aA	413.07 aA	450.54 bA
C. sinensis	121.18 aA	99.57 cA	480.26 aA	313.88 cB
P. calleryana	102.38 aB	169.90 aA	261.24 bA	362.30 cA
CV (%)	35.44		26.33	

Cultivars	Lipid peroxidation rootstock (uM MDA/g MF)		Lipid peroxidation graft (uM MDA/g MF)	
	P. calleryana	*C. sinensis*	*P. calleryana*	*C. sinensis*
Triunfo	426.66 a B	564.23 aA	183.33 cA	203.45 cA
Primorosa	418.33 aA	398.71 bA	141.53 dA	160.25 cA
Packham's Triumph	316.02 bA	340.12 bA	232.43 cA	209.74 cA
William's	558.07 aA	414.35 bB	223.84 cA	186.15 cA
Shenseri	472.18 aA	349.22 bB	120.89 dA	110.25 cA
Mendoza Inta 37	330.51 bA	353.71 bA	360.44 bA	263.71 bB
C. sinensis	468.97 aA	440.76 bA	514.74 aA	540.25 aA
P. calleryana	380.12 bA	423.33 bA	350.12 bA	298.59 bA
CV (%)	30.2		34.2	

* The averages followed by the same lowercase letter in the column and uppercase in the row within each variable belong to the same group by the Scott-Knott test at the 5% probability level

A significant interaction between scion and rootstock was also detected for hydrogen peroxide (H_2O_2) and lipid peroxidation (MDA) (Table 2).

In the rootstock portion of *P. calleryana*, no significant differences were observed among scions. Conversely, in *C. sinensis*, the highest H_2O_2 levels occurred in 'Primorosa' and 'Mendoza Inta 37', while 'William's' and the *C. sinensis* self-graft showed the lowest values. When comparing across rootstocks, *C. sinensis* tended to accumulate more H_2O_2 when grafted with *P. calleryana* or 'Primorosa'.

In the scion portion, grafts on *P. calleryana* exhibited higher H_2O_2 concentrations for 'Shenseri', 'Primorosa', *C. sinensis*, 'Triunfo', and 'Mendoza Inta 37'. On *C. sinensis*, 'Shenseri' showed the highest accumulation. The *C. sinensis* self-graft consistently presented the lowest H_2O_2 values among all scions, regardless of the rootstock (Table 2).

Lipid peroxidation (MDA) in the rootstock was highest for 'William's', 'Shenseri', *C. sinensis*, 'Triunfo', and 'Primorosa' grafted onto *P. calleryana*, whereas in *C. sinensis*, 'Triunfo' induced the greatest peroxidation. Overall, 'Triunfo' led to stronger lipid peroxidation in *C. sinensis*, while 'William's' and 'Shenseri' did so in *P. calleryana*.

In the scion portion, *C. sinensis* grafted onto *P. calleryana* displayed the highest lipid peroxidation, while 'Primorosa' and 'Shenseri' showed the lowest levels. On *C. sinensis*, the self-graft had the greatest peroxidation, followed by *P. calleryana* and 'Mendoza Inta 37'. Overall, 'Mendoza Inta 37' induced increased lipid peroxidation on *P. calleryana*, with no significant variation among the remaining scions.

Despite these variations, the hydrogen peroxide and lipid peroxidation profiles did not clearly distinguish compatible from incompatible combinations. For instance, *P. calleryana*, which failed to sprout on *C. sinensis*, exhibited similar H_2O_2 levels to the *C. sinensis* self-graft. Likewise, the cultivar 'Triunfo' showed high vigor on *P. calleryana* compared with *C. sinensis*, yet without corresponding differences in H_2O_2 concentration. Only lipid peroxidation in the *C. sinensis* rootstock was significantly higher than in *P. calleryana*, suggesting that ROS accumulation and oxidative stress intensity were not decisive factors in determining graft compatibility.

Anatomical analyses revealed that cell proliferation began as early as 5 days after grafting in 'Packham's Triumph' on *C. sinensis* (Fig. 1A). At 25 days, a distinct vascular connection was visible in the 'Primorosa'/*P. calleryana* combination (Fig. 1B). In contrast, the *C. sinensis*/*P. calleryana* graft exhibited poor adhesion and a necrotic barrier at the interface (Fig. 1C). The *P. calleryana* self-graft (Fig. 1D) displayed full bud sprouting and a continuous vascular bridge between scion and rootstock.

Callus formation initiated within 5 days for most cultivars (Fig. 2A, D and H), becoming measurable after 15 days in 'Mendoza Inta 37' (Fig. 2F). In 'Shenseri' and *P. calleryana* (Fig. 2E and G), callus tissue was already visible

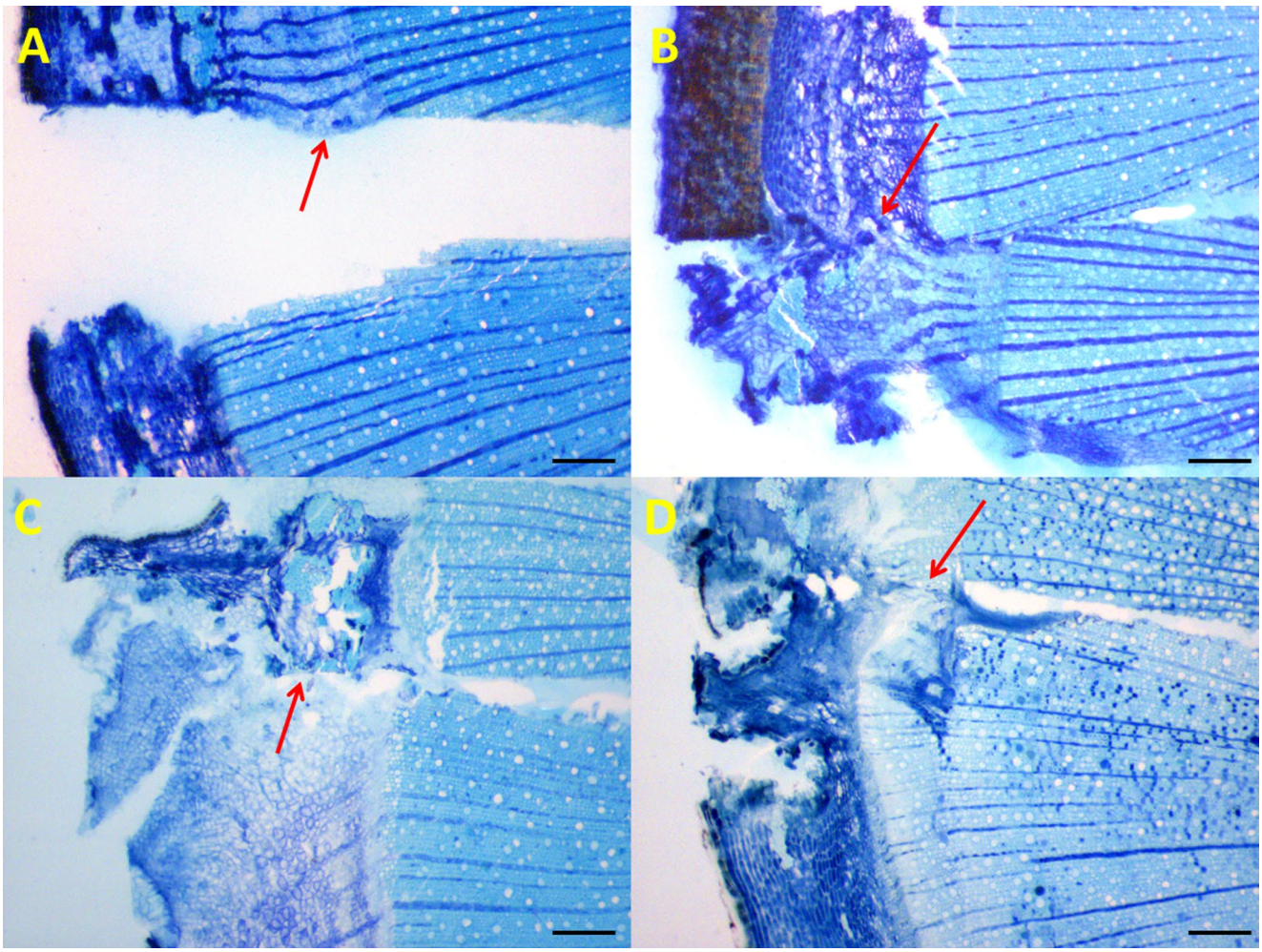


Fig. 1 Transverse sections in the graft region. Packham's Triumph on *Chaenomeles sinensis* at 5 days after grafting (**A**). Primorosa over *Pyrus calleryana* at 25 days after grafting (**B**). *Chaenomeles sinensis* on *Pyrus calleryana* at 45 days after grafting (**C**). *Pyrus calleryana* on *Pyrus caleryana* at 45 days after grafting (**D**). Bar = 200 µm

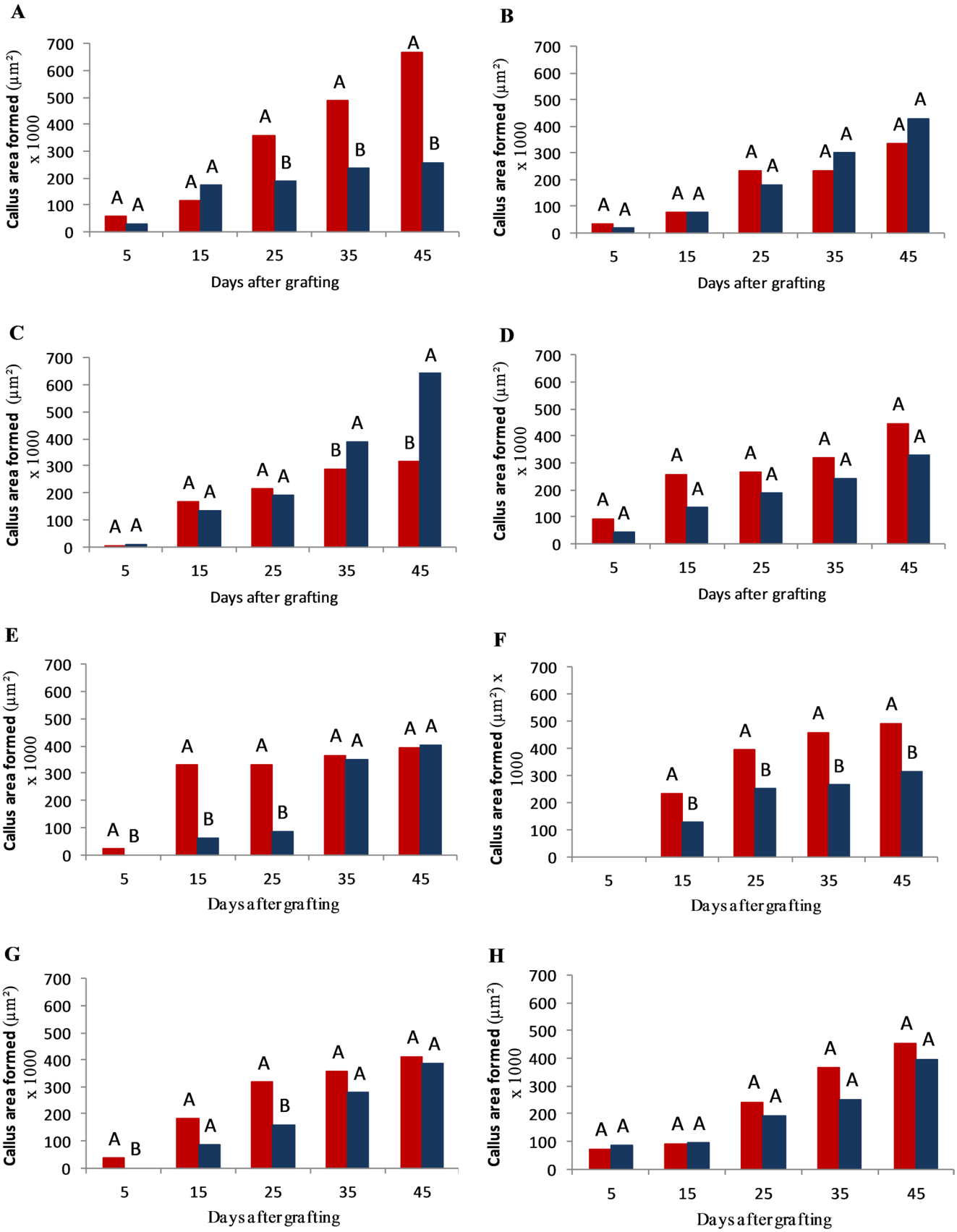


Fig. 2 Callus area formed in the grafting region over time after grafting from Packham's Triumph (**A**), William's (**B**), Triumph (**C**), Primorosa (**D**), Shenseri (**E**), Mendoza Inta crowns 37 (**F**), *P. caleryana* (**G**) and *C. sinensis* (**H**) in µm², in the *P. caleryana* (Blue) and *C. sinensis* (Red) rootstocks

on *C. sinensis* at 5 days, but quantification on *P. calleryana* was only possible after 15 days. Callus proliferation showed high variability among combinations, progressively filling the interface region.

For 'Packham's Triumph', callus area did not differ between rootstocks up to 15 days, but by 45 days, callus mass was significantly larger on *C. sinensis*. The cultivar 'Mendoza Inta 37' also showed greater callus formation on *C. sinensis* across all evaluations.

Regarding bark thickness (Fig. 3), 'Packham's Triumph' displayed the highest values, while 'Primorosa', 'William's', 'Shenseri', 'Triunfo', and *P. calleryana* did not differ significantly.

Correlation analyses (Fig. 4) demonstrated that in *C. sinensis*, shoot length, diameter, and canopy lipid peroxidation were positively correlated, suggesting that moderate oxidative activity may accompany vigorous shoot growth. In *P. calleryana*, however, lipid peroxidation correlated negatively with bud diameter, consistent with the inhibitory effect of excessive membrane damage on tissue expansion. Other variables showed no significant correlations, confirming that graft compatibility results from multiple interdependent factors, including biochemical and anatomical dynamics that are not easily isolated.

Discussion

Graft compatibility emerges from a finely tuned coordination between intercellular signaling, redox metabolism, and vascular differentiation at the graft interface. The methodological integration of anatomical observations with physiological and growth-related variables allowed a direct association between vascular continuity and redox homeostasis, providing a mechanistic explanation for the differences observed among graft combinations. The anatomical patterns observed in the present study align with the notion that successful grafting depends not only on physical contact but also on effective signaling networks that regulate cell differentiation and vascular reconnection (Liu et al. 2023a, b; Wang et al. 2024). In a comparative study involving pear and quince trees grafted onto *Pyrus calleryana* and *Cydonia sinensis* rootstocks, Melo et al. (2017) found greater compatibility between pear and *P. calleryana* and between quince and *C. sinensis*, a pattern also supported by Pio et al. (2007). These results reinforce the hypothesis that interspecific affinity is largely determined by the ability of graft partners to establish coordinated communication during the healing process.

At the cellular level, compatible combinations exhibit continuous vascular differentiation driven by coordinated

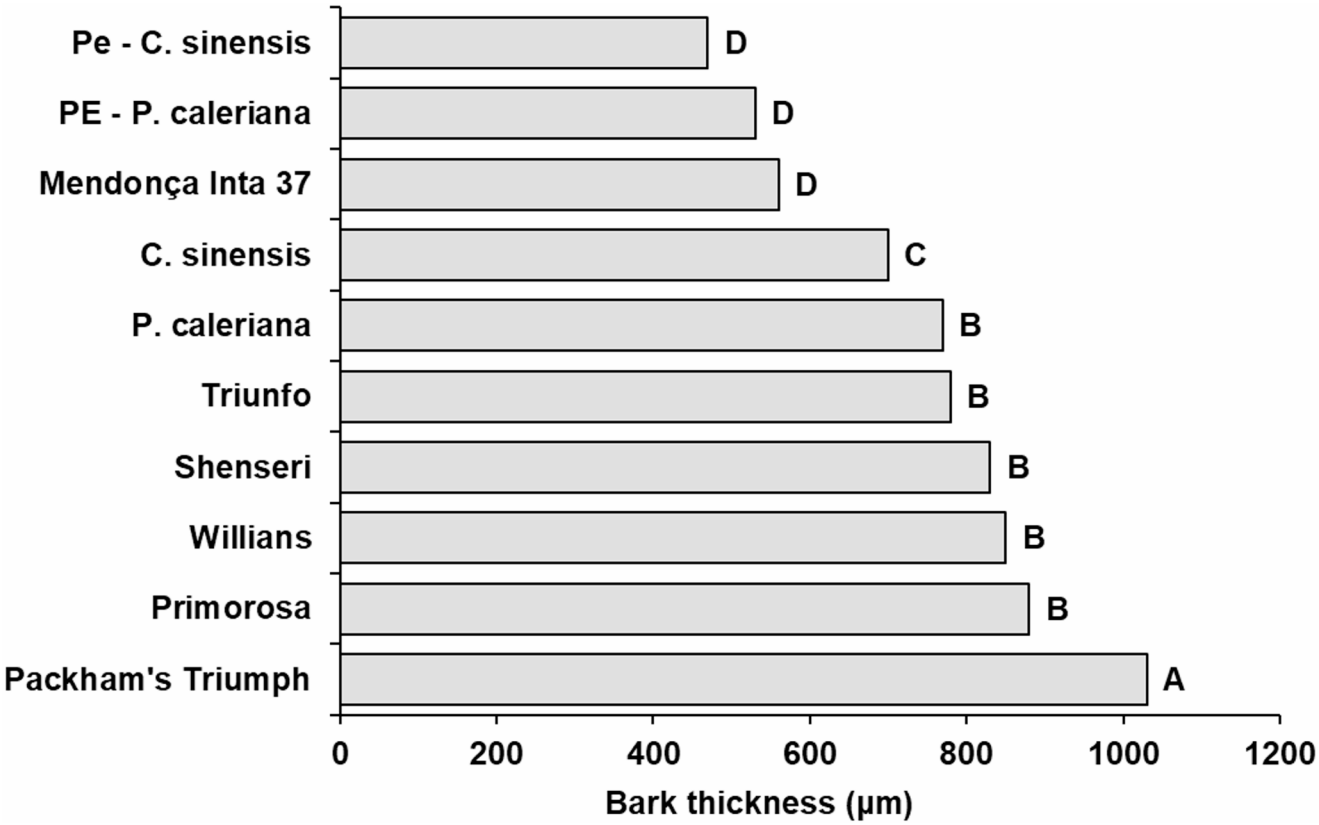


Fig. 3 Bark thickness in (µm) of the Packham's Triumph, William's, Triunfo, Primorosa, Shenseri, Mendoza Inta 37, *P. caleryana* and *C. sinensis* and rootstocks *P. caleryana* (PE – *Pyrus*) and *C. sinensis* (PE – *Chaenomeles*)

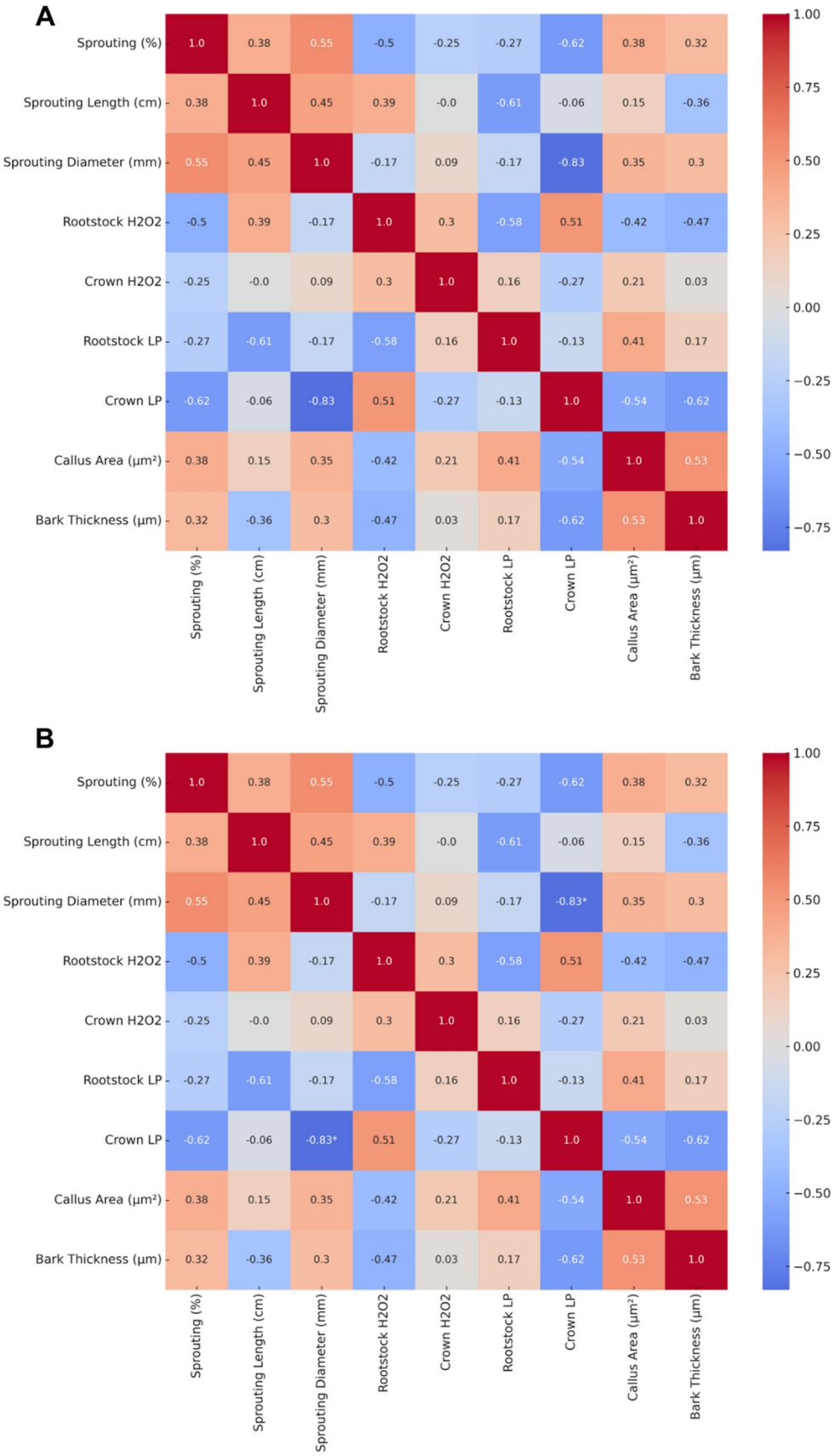


Fig. 4 A. Pearson correlation coefficient for the roorstock *C. sinensis*. **B**. Pearson correlation coefficient for the roorstock *P. caleryana*

hormonal and redox signaling (Öztürk 2021; Adhikari et al. 2022). Auxin plays a central role in this process, guiding cell polarity and xylem formation across the graft interface. Rapid activation of genes involved in auxin transport, lignin biosynthesis, and cell wall remodeling has been reported in compatible grafts, whereas incompatible pairs often show impaired auxin flow and accumulation of phenolic compounds that disrupt cell-to-cell communication (Habibi et al. 2022; Ji et al. 2022). This is consistent with the patterns observed in our study, where compatible grafts displayed organized callus proliferation and early vascular reconnection, while incompatible combinations exhibited discontinuities and localized necrosis.

The role of reactive oxygen species (ROS) in graft healing is dual and tightly regulated. Moderate ROS accumulation serves as a signaling cue for cell wall loosening and defense activation, whereas excessive ROS leads to oxidative damage and cellular dysfunction (Amri et al. 2021). Our findings indicate that lipid peroxidation levels, although variable among combinations, did not consistently discriminate compatibility status, reinforcing that oxidative imbalance alone is insufficient to explain graft failure without anatomical context.

Rather than acting as isolated stress indicators, H_2O_2 and MDA functioned as complementary markers of graft performance when interpreted together with anatomical continuity and shoot development. The preferential accumulation of H_2O_2 in scion tissues suggests a dominant role of ROS as signaling molecules regulating vascular regeneration and cell differentiation at the graft interface. In contrast, the higher MDA levels in rootstocks indicate increased lipid peroxidation and membrane destabilization, reflecting a greater oxidative burden associated with structural maintenance under graft-induced stress. The elevated absolute values compared with those reported by Nocito et al. (2010) may reflect the use of differentiated tissues in our study, which exhibit higher metabolic activity and compartmentalized redox regulation (Kapazoglou et al. 2021). ROS are also known to modulate auxin transport by regulating PIN protein localization and activity, thereby coordinating redox status with polar auxin flow and vascular strand formation at the graft interface.

Callus formation represents one of the earliest and most visible outcomes of successful signaling between the graft partners. In our observations, the phloem and cortical regions were the main sources of callogenic tissue, corroborating Balbi et al. (2019). Differences in the timing and extent of callus proliferation between combination such as the early callus formation observed in ‘Shenseri’ onto *P. calleryana* compared with *C. sinensis* highlight the species-specific responses to wound-induced hormonal cues (Wang et al. 2024; Tunç et al. 2025). Auxin gradients, together with cytokinin and jasmonate signaling, are thought to coordinate the reprogramming of cells toward a regenerative state, enabling the establishment of functional vasculares bridges (Wang et al. 2024). Anatomical evaluation was not merely descriptive, but functioned as a validation layer for the physiological results, as combinations that exhibited early vascular reconnection consistently showed superior growth and more stable redox profiles.

Anatomical evidence from this and previous studies suggests that graft adhesion and compatibility depend on the synchronized differentiation of xylem and phloem tissues (Adhikari et al. 2022). In incompatible combinations, failure to re-establish this vascular continuity likely results from disrupted signaling between the cambial regions and increased accumulation of inhibitory phenolics (Habibi et al. 2022; Parisi et al. 2023). Such accumulation may interfere with auxin perception and reactive oxygen metabolism, reinforcing a feedback loop of incompatibility. These processes underscore the importance of biochemical communication in the success or failure of graft formation. In compatible combinations, anatomical sections revealed the progressive establishment of cambial continuity, with newly differentiated xylem and phloem forming continuous vascular bridges across the graft interface. Parenchyma cell proliferation played a central role in connecting the scion and rootstock tissues, while gradual reorganization of the cortical region ensured structural integration. In contrast, incompatible grafts frequently developed necrotic layers at the interface, preventing vascular continuity and forming an isolation barrier that restricted nutrient transport and signal exchange.

The significant correlations observed between shoot length, stem diameter, and lipid peroxidation levels further support the interaction between structural and signaling processes. Cellular damage derived from oxidative imbalance directly limits growth and resource allocation, linking morpho-anatomical traits to molecular stress responses (Loupit et al. 2023; Feng et al. 2024). These correlations may serve as indirect indicators of the efficiency of signal transduction across the graft interface, particularly in combinations where hormonal or metabolic dialogue is impaired.

Altogether, our findings support the idea that graft compatibility in *Cydonia* and *Pyrus* species results from integrated hormonal, redox, and metabolic signaling that orchestrates callus formation and vascular reconnection (Wang et al. 2024). Future studies should focus on quantifying antioxidant enzymes such as superoxide dismutase (SOD), catalase (CAT), and peroxidases (POX), as well as profiling auxin levels and expression of its transport-related gene families (PIN and AUX/LAX). In addition, the investigation of ROS producing enzymes such as respiratory burst oxidase homologs (RBOH) and genes associated

with the phenylpropanoid pathway may provide insight into molecular thresholds that determine graft success or failure (Aluko et al. 2025). Integrating transcriptomic approaches with targeted hormone profiling and vascular imaging will substantially improve early diagnosis of graft compatibility in woody species.

Our anatomical and biochemical temporal analyses support a model in which controlled ROS accumulation functions as an upstream regulator of auxin-mediated vascular differentiation, linking redox homeostasis to developmental regulation of the graft union (Parveen et al. 2022; Pasternak et al. 2023). This framework positions oxidative metabolism not merely as a stress response, but as an active physiological process governing tissue integration and functional reconnection. Future studies combining transcriptomic profiling, hormone quantification, and vascular imaging will be essential to validate this model and define molecular thresholds that differentiate compatible from incompatible graft interactions.

Conclusion

The results demonstrate that vascular reconnection and early shoot growth in pear and quince grafts are closely associated with regulated oxidative metabolism at the graft interface. Compatible combinations were able to balance ROS production and cellular protection, ensuring continuous vascular differentiation and organ development. In contrast, incompatible pairs exhibited anatomical discontinuity and stress-associated damage. Therefore, ROS act not simply as stress agents, but as developmental signals that guide healing and tissue integration. Future approaches combining redox markers with hormonal regulation and gene expression may allow earlier and more accurate prediction of graft compatibility, with direct applications to the propagation of woody fruit species.

Funding The Article Processing Charge (APC) for the publication of this research was funded by the Coordenação de Aperfeiçoamento de Pessoal de Nível Superior - Brasil (CAPES) (ROR identifier: 00x0ma614).

Open Access This article is licensed under a Creative Commons Attribution 4.0 International License, which permits use, sharing, adaptation, distribution and reproduction in any medium or format, as long as you give appropriate credit to the original author(s) and the source, provide a link to the Creative Commons licence, and indicate if changes were made. The images or other third party material in this article are included in the article's Creative Commons licence, unless indicated otherwise in a credit line to the material. If material is not included in the article's Creative Commons licence and your intended use is not permitted by statutory regulation or exceeds the permitted use, you will need to obtain permission directly from the copyright holder. To view a copy of this licence, visit http://creativecommons.org/licenses/by/4.0/.

References

Adhikari PB, Xu Q, Notaguchi M (2022) Compatible graft establishment in fruit trees and its potential markers. Agron 12(8):1981. https://doi.org/10.3390/agronomy12081981

Aluko OO, Ninkuu V, Jianpei Y, Chen S, Zeng H, Dakurah FD (2025) Phenylpropanoids metabolism: recent insight into stress tolerance and plant development cues. Front Plant Sci 16:1571825. https://doi.org/10.3389/fpls.2025.1571825

Amri R, Font i Forcada C, Giménez R, Pina A, Moreno MÁ (2021) Biochemical characterization and differential expression of PAL genes associated with "translocated" peach/plum graft-incompatibility. Front Plant Sci 12:622578. https://doi.org/10.3389/fpls.2021.622578

Anjum NA, Gill SS, Corpas FJ, Ortega-Villasante C, Hernandez LE, Tuteja N, Fujita M (2022) Recent insights into the double role of hydrogen peroxide in plants. Front Plant Sci 13:843274. https://doi.org/10.3389/fpls.2022.843274

Ashraf I, Cipriani G, De Mori G (2025) Bridging the gap: genetic insights into graft compatibility for enhanced Kiwifruit production. Int J Mol Sci 26(7):2925. https://doi.org/10.3390/ijms26072925

Buege JA, Aust SD (1978) Microsomal lipid peroxidation. Methods in enzymology, vol 52. Academic press, pp 302–310

Darshan D, Solanki SPS (2022) Rootstock problem and their influence in temperate fruit crops. Planta 4:912–932

Feng M, Augstein F, Kareem A, Melnyk CW (2024) Plant grafting: molecular mechanisms and applications. Mol Plant 17(1):75–91. https://doi.org/10.1016/j.molp.2023.12.006

Ferreira DF (2019) Sisvar: Um sistema de análise computadorizada Para Projetos do Tipo split plot de Efeitos Fixos. Rev Bras Biom 37:529–535. https://doi.org/10.28951/rbb.v37i4.450

Habibi F, Liu T, Folta K, Sarkhosh A (2022) Physiological, biochemical, and molecular aspects of grafting in fruit trees. Hortic Res 9:uhac032. https://doi.org/10.1093/hr/uhac032

Hong Y, Boiti A, Vallone D, Foulkes NS (2024) Reactive oxygen species signaling and oxidative stress: transcriptional regulation and evolution. Antioxidants 13(3):312. https://doi.org/10.3390/antiox13030312

Ji P, Liang C, Yang Y, Wang R, Wang Y, Yuan M, Qiu Z, Cheng Y, Liu J, Li D (2022) Comparisons of anatomical characteristics and transcriptomic differences between heterografts and homografts in *Pyrus* L. Plants 11(5):580. https://doi.org/10.3390/plants11050580

Kapazoglou A, Tani E, Avramidou EV, Abraham EM, Gerakari M, Megariti S, Doulis AG (2021) Epigenetic changes and transcriptional reprogramming upon woody plant grafting for crop sustainability in a changing environment. Front Plant Sci 11:613004. https://doi.org/10.3389/fpls.2020.613004

Kraus JE, Arduin M (1997) Manual básico de métodos em morfologia vegetal. EDUR, Rio de Janeiro

Kurt T, Öztürk A, Faızı ZA, Polat Y (2023) Effects of quince rootstocks and pear cultivars on fruit and yield characteristics. Yuzuncu Yıl Univ J Agricultural Sci 33(2):288–297. https://doi.org/10.29133/yyutbd.1263145

Liu Q, Wang X, Zhao Y, Xiao F, Yang Y (2023a) Transcriptome and physiological analyses reveal new insights into delayed incompatibility formed by interspecific grafting. Sci Rep 13(1):4574. https://doi.org/10.1038/s41598-023-31804-4

Liu Y, Liu H, Zhang T, Liu J, Sun X, Sun X, Zheng C (2023b) Interactions between rootstock and scion during grafting and their molecular regulation mechanism. Sci Hortic 308:111554. https://doi.org/10.1016/j.scienta.2022.111554

Loupit G, Brocard L, Ollat N, Cookson SJ (2023) Grafting in plants: recent discoveries and new applications. J Exp Bot 74(8):2433–2447. https://doi.org/10.1093/jxb/erad061

Melo ETD, Pio R, Balbi RV, Ferreira CA, Mori FA (2017) Anatomic compatibility of pear and quince trees grafted on *Pyrus calleryana* and *Chaenomeles sinensis* rootstocks. Pesqui Agropecu Bras 52(10):877–886. https://doi.org/10.1590/S0100-204X2017001000007

Milagres CH, Fazenda LHV, da Silva AD, Peche PM, dos Santos LDJ, Pio R, Mori FA (2023) Methods of adventitious rooting of rootstocks for quince trees. Rhizosphere 25:100662. https://doi.org/10.1016/j.rhisph.2023.100662

Nie W, Wen D (2023) Study on the applications and regulatory mechanisms of grafting on vegetables. Plants 12(15):2822. https://doi.org/10.3390/plants12152822

Nocito FF, Espen L, Fedeli C, Lancilli C, Musacchi S, Serra S, Sacchi GA (2010) Oxidative stress and senescence-like status of pear calli co-cultured on suspensions of incompatible quince microcalli. Tree Physiol 30(4):450–458. https://doi.org/10.1093/treephys/tpq006

Ozturk A, Faizi ZA (2023) Growth, yield and quality performance of pear (*Pyrus communis* L.) cv.'Santa Maria'under high density planting. Braz Arch Biol Technol 66:e23220414. https://doi.org/10.1590/1678-4324-2023220414

Öztürk A (2021) The effects of different rootstocks on the graft success and stion development of some pear cultivars. Int J Fruit Sci 21(1):932–944. https://doi.org/10.1080/15538362.2021.1948376

Parisi M, Pentangelo A, D'Alessandro A, Festa G, Francese G, Navarro A, Mennella G (2023) Grafting effects on bioactive compounds, chemical and agronomic traits of 'Corbarino'tomato grown under greenhouse healthy conditions. Hortic Plant J 9(2):273–284. https://doi.org/10.1016/j.hpj.2022.03.001

Parveen N, Kandhol N, Sharma S, Singh VP, Chauhan DK, Ludwig-Müller J, Tripathi DK (2022) Auxin crosstalk with reactive oxygen and nitrogen species in plant development and abiotic stress. Plant Cell Physiol 63(12):1814–1825. https://doi.org/10.1093/pcp/pcac138

Pasternak T, Palme K, Pérez-Pérez JM (2023) Role of reactive oxygen species in the modulation of auxin flux and root development in Arabidopsis Thaliana. Plant J 114(1):83–95. https://doi.org/10.1111/tpj.16118

Pio R, Chagas EA, Barbosa W, Tombolato AFC, Signorini G (2007) Intergeneric grafting of pear cultivars to the'japonês'quince tree. In X International Pear Symposium 800 (pp. 707–712). https://doi.org/10.17660/ActaHortic.2008.800.96

Seifert KE, Pio R, Celant VM, Chagas EA (2009) Mudas de Pera produzidas Por dupla enxertia Em Marmeleiro utilizando o Porta-enxerto 'Japonês.' Pesqui Agropecu Bras 44:1631–1635. https://doi.org/10.1590/S0100-204X2009001200010

Tan Y, Duan Y, Chi Q, Wang R, Yin Y, Cui D, Sun H (2023) The role of reactive oxygen species in plant response to radiation. Int J Mol Sci 24(4):3346. https://doi.org/10.3390/ijms24043346

Tunç Y, Yılmaz KU, Khadivi A (2025) Evaluation of graft compatibility in some wild olive *(Olea europaea* L. subsp. oleaster) genotypes selected in the Eastern Mediterranean region. BMC Plant Biol 25(1):346. https://doi.org/10.1186/s12870-025-06344-w

Velikova V, Yordanov I, Edreva A (2000) Oxidative stress and some antioxidant systems in acid rain-treated bean plants: protective role of exogenous polyamines. Plant Sci 151(1):59–66. https://doi.org/10.1016/S0168-9452(99)00197-1

Wang L, Liao Y, Liu J, Zhao T, Jia L, Chen Z (2024) Advances in understanding the graft healing mechanism: a review of factors and regulatory pathways. Hortic Res 11(8):uhae175. https://doi.org/10.1093/hr/uhae175

Wang T, Jin Z, Yuan Y, Deng L, Sun G, He S, Wang Z (2025) Interstock-mediated graft incompatibility: insights into photosynthetic pigments, carbohydrates, antioxidant defense systems, and hormones response mechanisms in citrus. Plants 14(4):522. https://doi.org/10.3390/plants14040522

Yuan D, Wu X, Jiang X, Gong B, Gao H (2024) Types of membrane transporters and the mechanisms of interaction between them and reactive oxygen species in plants. Antioxidants 13(2):221. https://doi.org/10.3390/antiox13020221

Publisher's Note Springer Nature remains neutral with regard to jurisdictional claims in published maps and institutional affiliations.